Fire Simulations of a Container Ship with FRP Structures

Tuula Hakkarainen
VTT Technical Research Centre of
Finland Ltd
Espoo, Finland
tuula.hakkarainen@vtt.fi

Alexandra Viitanen
VTT Technical Research Centre of
Finland Ltd
Espoo, Finland
alexandra.viitanen@vtt.fi

Timo Korhonen
VTT Technical Research Centre of
Finland Ltd
Espoo, Finland
timo.korhonen@vtt.fi

Terhi Kling
VTT Technical Research Centre of
Finland Ltd
Espoo, Finland
terhi.kling@vtt.fi

Antti Korkealaakso
VTT Technical Research Centre of
Finland Ltd
Espoo, Finland
antti.korkealaakso@vtt.fi

Abstract—**Fire simulations of a container ship with fibre-reinforced polymer (FRP) structures have been performed. The fire safety effect of using FRP as the primary construction material of the vessel was studied, compared to conventional steel structures. The effect of FRP structures on fire development was assessed by comparing the simulated gas temperatures and heat release rates with FRP and steel structures. The effect of protective mineral wool and intumescent coating layers was quantified. The simulation results highlight that FRP structures present a significant fire load by themselves, and should be well protected. Mineral wool was found to be better protection than the intumescent coating: it can either prevent or postpone the pyrolysis of the FRP bulkhead, depending on the fire exposure. Early detection and containment of the fire are of high importance for preventing fire spread.**

Keywords—fire simulation, pyrolysis modelling, FRP structures, container ship

I. Introduction

The European FIBRESHIP project (2017–2020) aimed at developing a new market focused on the construction of commercial vessels greater than 50 m in length in composite materials (Fibre-Reinforced Polymers, FRP). Its main objective was to generate the regulatory framework that allows the designing and building of large-length ships in FRP material overcoming the technical challenges identified. In order to achieve this objective, the project qualified and audited innovative FRP materials for marine applications, elaborated new designs and production guidelines, generated production and inspection methodologies, and developed numerical software tools capable of assessing the structural performance validated through experimental testing.

As a part of the workpackage devoted to design, engineering and development of guidelines, onboard fire events were simulated to assess the fire safety effect of using FRP as the primary construction material of the vessel, compared to conventional steel structures. This paper describes the fire simulations of a container ship with FRP structures. Several fire scenarios inside the superstructure of a 4250 twenty-foot equivalent unit (TEU) container vessel were simulated with a computational fluid dynamics (CFD) software Fire Dynamics Simulator (FDS), version 6.7.1 [1]. First, the simulation input including geometry, surfaces, material models, fire scenarios and design fires, ventilation,

and instrumentation is introduced. Next, the simulation results are presented and analysed. Finally, the practical significance of the results is discussed and conclusions are drawn.

From the fire safety aspect, the effect of FRP structures on the fire development was of primary interest. It was assessed by comparing the results from simulations with FRP structures to the results from reference simulations where all structures were conventional steel structures. Furthermore, the effect of protective mineral wool and intumescent coating layers was quantified.

In addition, one objective of this study was to gain better understanding of simulating enclosure fires with FRP structures. The main challenge was to define the pyrolysis model for FRP. It is to be noted that pyrolysis modelling of complex materials, simulating fires including structural responses or simulating ventilation-controlled enclosure fires are not by any means mature. The results of this study are thus limited in application.

II. Simulation Input

A. Geometry

The simulation model consisted of multiple spaces located on the same superstructure deck. The simulated geometry was a simplified version of the container vessel's deck D, with some of the spaces neglected in the simulation model. The simulated spaces included a corridor, cabins, a crew dayroom and a laundry room. The model had a length of 12.0 m, a width of 23.2 m and a height of 2.8 m, which were based on the ship's general arrangement. The computational meshes were divided into 10 cm cubical cells. Visualization of the model geometry with dimensions is shown in Fig. 1. Doors leading to the individual spaces were included in the model and are shown in white in Fig. 1. Each door had a width of 0.8 m and a height of 2.0 m.

Due to the enclosed nature of the space, the available oxygen limits the size of the fire in terms of heat release. To alter the maximum heat release, natural ventilation was increased in some of the simulations by adding either one or two open doors. In the simulation with one open door, the door connecting the laundry room to the corridor was open. In the simulation with two open doors, the door to open deck at the portside end of the corridor was also open in addition to the door connecting the laundry room and the corridor.
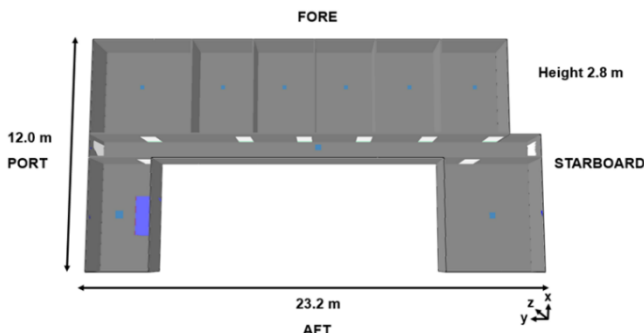
Fig. 1. Model geometry (floor plan) with dimensions. Positions of design fire, air supplies below ceiling and doors are shown in blue, light blue and white, respectively.

B. Surfaces

Two different primary bulkhead materials were used in the simulations, steel and FRP. Insulation materials were used with the primary construction materials in the simulation. The decks below and above the spaces were steel structures in all simulations.

All steel structures were defined as sandwich structures consisting of three layers. The external layers were steel and the core was mineral wool. The thickness of the steel layers was 2 mm each, and the mineral wool layer was 6 cm thick.

The FRP bulkheads were similarly defined to be sandwich structures with three layers. The external layers were FRP material with the trade name of SAERTEX LEO®. The core of the sandwich was mineral wool. The FRP layers were 2.9 mm thick each and the mineral wool core was 4.4 cm thick. The protective layer was either an additional external layer of mineral wool with a thickness of 6 cm or an external layer of intumescent coating with a thickness of 2 mm. Intumescent coating was used inside the spaces with negligible fire load, i.e., the corridor, and on the exterior bulkheads. On other bulkheads, mineral wool was used for insulation.

The conditions outside the superstructure were considered ambient, i.e., the external sides of the bulkheads were constantly transferring heat to the ambient air. The ambient temperature in the simulations was defined to be 20 °C.

C. Material models

The required material properties for the simulations included density, conductivity, specific heat and emissivity. As the fibre-reinforced polymer was assumed to thermally decompose in the simulations due to the elevated temperatures, a pyrolysis model was needed in addition to the material properties.

1) Steel

The material properties used for steel corresponded to the properties given for stainless steel in the Eurocode 3 [2], which is the harmonised European standard for design of steel structures.

2) Mineral wool

The material properties used for mineral wool corresponded to general-type stone wool. Material properties for such materials are presented for example in [3].

3) Fibre-reinforced polymer

The FRP material properties and the pyrolysis model were based on the experimental results acquired during the FIBRESHIP project, presented in [4]. The development of the material model followed the modelling principles presented in [5].

The fibre-reinforced polymer was modelled as consisting of vinyl ester resin, glass fibre and moisture. The mass of FRP material was assumed to consist of 23.75 % of vinyl ester resin, 1.25 % of moisture and 75 % of glass fibre.

The vinyl ester resin was assumed to consist of two components based on the small-scale thermogravimetric analysis (TGA). The mass of the vinyl ester resin was assumed to consist of 42 % of the first resin component and 58 % of the second resin component.

The material properties of the vinyl ester resin components were assumed the same. The material properties of FRP components are presented in Table I.

TABLE I. MATERIAL PROPERTIES OF COMPONENTS OF FIBRE-REINFORCED POLYMER

Resin Components 1 and 2	
Emissivity	0.9
Density	1000 kg/m³
Specific heat	2.152 kJ/kgK
Conductivity	0.25 W/mK
Glass fibre	
Emissivity	0.9
Density	2400 kg/m³
Specific heat	1.2 kJ/kgK
Conductivity	0.65 W/mK
Moisture	
Emissivity	0.9
Density	1000 kg/m³
Specific heat	4.0 kJ/kgK
Conductivity	1.2 W/mK

The resin components were assumed to pyrolyse in elevated temperatures. The complex pyrolysis model of FDS was utilized to model the thermal degradation of the material [1]. A simplified presentation of the assumed pyrolysis reaction mechanisms is shown in Table II. The reaction rates are dependent on the temperature, and some of the reactions are oxidative, i.e., the reaction rates are dependent on the local oxygen concentration. The produced fuel gas was assumed to be propane, which has heat of combustion of ca. 44.4 MJ/kg. The produced inert gas was assumed to be water vapour.

TABLE II. REACTION MECHANISMS OF RESIN COMPONENTS

Component	Reaction No.	Products (Yield %)
Component 1	1	Solid product 1 (10 %) Fuel gas (90 %)
	2	Solid product 1 (80 %) Fuel gas (20 %)
Component 2	1	Solid product 1 (20 %) Fuel gas (80 %)
Solid product 1	1	Solid product 2 (8 %) Fuel gas (92 %)
Solid product 2	–	–

Cone calorimeter test results, for both a vinyl ester resin specimen (cured resin) and a specimen consisting of vinyl ester resin and glass fibre (laminate) were utilized to manually estimate the material properties for the glass fibre, the assumed resin components and their solid pyrolysis products. The experimentally measured density was used as a boundary value for the estimated component densities. The material properties were evaluated using expert judgement and similar reference materials to ensure that realistic values were used.

Regarding the assumptions made about the other components of FRP material, moisture changes phase into water vapour in elevated temperatures. The glass fibre was not considered reactive.

4) Intumescent coating

The material properties and the pyrolysis model for the intumescent coating were based on the experimental results acquired during the FIBRESHIP project [4]. The development of the material model follows the modelling principles presented in [5].

The intumescent coating was assumed to consist of two components based on the TGA results, presented in [4]. The material properties of the intumescent coating components were assumed the same and are presented in Table III.

TABLE III.   MATERIAL PROPERTIES OF INTUMESCENT COATING COMPONENTS

Intumescent Coating Components	
Emissivity	1.0
Density	1500 kg/m^3
Specific heat	1.0 kJ/kgK
Conductivity	0.6 W/mK

The intumescent coating components were assumed to pyrolyse in elevated temperatures. The complex pyrolysis model of FDS was utilized to model the thermal degradation of the material [1]. A simplified presentation of the assumed pyrolysis reaction mechanisms is shown in Table IV. The produced fuel gas was assumed to be propane, which has heat of combustion of ca. 44.4 MJ/kg. The produced inert gas was assumed to be water vapour.

TABLE IV.   REACTION MECHANISMS OF INTUMESCENT COATING COMPONENTS

Component	Reaction No.	Products (Yield %)
Component 1	1	Inert gas (100 %)
Component 2	1	Solid product 1 (94.6 %) Inert gas (5.4 %)
Solid product 1	1	Solid product 2 (40 %) Fuel gas (60 %)
	2	Solid product 3 (90 %) Fuel gas (10 %)
Solid product 2	1	Solid product 4 (50 %) Fuel gas (50 %)
	2	Solid product 5 (85 %) Fuel gas (15 %)
Solid product 3	1	Solid product 5 (10 %) Fuel gas (90 %)
	2	Solid product 4 (50 %) Fuel gas (50 %)
Solid product 4	–	–
Solid product 5	1	Inert gas (50 %) Solid product 4 (50 %)

D. Fire scenarios and design fires

Twelve (12) different fire scenarios were simulated. The design fire, the primary bulkhead material and the natural ventilation were varied to produce the different fire scenarios. The simulated physical time was 60 min 10 s for all fire scenarios, presented in Table V.

In the simulations with FRP bulkheads, the FRP pyrolysed, i.e., generated fuel gas, after reaching sufficiently high temperature. The produced fuel gas ignited if there was enough oxygen available and the gas temperature was sufficiently high.

TABLE V.   SIMULATED FIRE SCENARIOS

Design fire	Bulkhead material	Natural ventilation
Towel rack fire in the middle of the starboard side in the laundry room	Steel	Doors closed, leakage
		Laundry door open, leakage
		Laundry door and portside external door open, leakage
	FRP	Doors closed, leakage
		Laundry door open, leakage
		Laundry door and portside external door open, leakage
Towel rack fire in the aft corner on the portside in the laundry room	Steel	Doors closed, leakage
		Laundry door open, leakage
		Laundry door and portside external door open, leakage
	FRP	Doors closed, leakage
		Laundry door open, leakage
		Laundry door and portside external door open, leakage

As the availability of oxygen affects the heat release rate, the ventilation conditions were also varied in the simulations. Each pair of a design fire and a primary bulkhead material was simulated with three different natural ventilations. The details of the ventilation modelling are presented in Section E.

A towel rack fire was utilized as a design fire in all simulations. The towel rack was presented in the simulations with a hexahedral geometry with a height of 1.6 m, a width of 2 m and a depth of 1 m. Depending on the simulation, the hexahedral geometry was located either in the middle of the longitudinal bulkhead on the starboard side or in the aft corner on the portside.

The heat release rate of the towel rack fire as a function of time is presented in Fig. 2. The heat release rate consists of growth, steady and decay phases. The heat release rate was applied as a boundary condition to the largest vertical surface of the hexahedron that was not facing the wall.

In simulations with FRP as the primary bulkhead construction material, the FRP bulkheads began to generate gaseous fuel after reaching a sufficiently high temperature. Their thermal degradation was modelled utilizing the pyrolysis model of FDS, with material properties presented above.
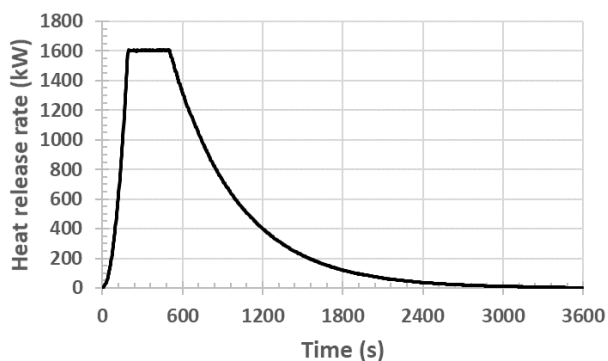
Fig. 2. Heat release rate of the towel rack fire.

E. Ventilation

The spaces were simulated as constantly mechanically ventilated. The HVAC (Heating, Ventilation, and Air Conditioning) submodule of FDS was utilized to model a complex ventilation system that is able to react to pressure changes caused by the fire. Each individual space had at least one air supply and one air exhaust in the simulation. The ventilation rates were estimated based on the design occupancies of the spaces and the minimum airflow rate per person as given in [6].

Three different natural ventilation conditions were utilized in the simulations. Either all doors between the individual spaces were kept closed, one door was open or two doors were open, as described in Section A.

Each closed door was assumed to have a leakage that was equivalent to a leak with an area of 0.023 m^2. For doors not connecting to the outside, the leakage was modelled using the localized leakage model implemented in FDS. With this approach, the energy of the gas could be preserved as it passed through the leak. With the pressure zone leakage model of FDS, which was used with closed external doors, there was no heat transport from the leaking enclosure. Furthermore, the localized leakage model uses the local gas pressure to determine the amount of leakage whereas the pressure zone leakage model uses the zone pressure. With the localized leakage model, the leaking area was assumed to be located low on the door panel. The leaking area was one gas cell above the bottom deck, had a height of one gas cell and had the same width as the door. With the pressure zone leakage model, the leakage was assumed to occur through the whole door panel. The assumed amount of leakage corresponded to structures that are considered relatively tight [3].

F. Instrumentation

Various quantities were monitored in the simulations, both at discrete points and at specific planes. The mass and volume flows in the HVAC system and through the leaks were also monitored. The following quantities were monitored:

- gas temperatures in each individual space, at least at one location, at heights of 55, 105, 140, 155 and 205 cm,
- pressures in each individual space, at least at one location, at height of 140 cm,
- gas temperatures and oxygen and carbon monoxide volume fractions at both transverse and longitudinal planes going through the domain,

- temperatures at the back of the bulkhead and burning rates at the solid boundaries,
- mass and volume flows separately for each localized leak and HVAC system duct.

III. SIMULATION RESULTS AND ANALYSIS

In this section, the results of the simulations are analysed on the basis of heat release rates (HRR), gas temperatures in the middle of the laundry at the height of 155 cm (Tgas_laundry5_z155cm), and gas temperatures in the corridor 5.8 m from the portside end at the height of 140 cm (Tgas_Corridor2). The primary bulkhead material in the simulations is either FRP or steel.

A. Fire in the middle of the starboard side

1) All doors closed

HRR, Tgas_laundry5_z155cm, and Tgas_Corridor2 values from both simulations with the design fire located in the middle of the starboard side and all doors closed are shown in Fig. 3.
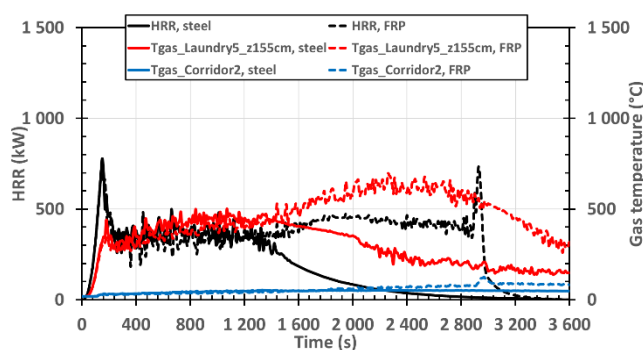

Fig. 3. Simulated HRR and gas temperature results, design fire in the middle of the starboard side, all doors closed.

During the first ca. 1300 s (ca. 22 min) of the simulation, the HRRs were very similar in both simulations. After this, the fire in the simulation with steel as primary bulkhead material began to decay according to the design fire curve. In the simulation with FRP as the primary bulkhead material, the FRP structures generated gaseous fuel, but it was unable to combust completely due to lack of oxygen. As the gas temperature in the laundry room was sufficiently high, the unburnt gaseous fuel continued to combust after the decay of the design fire.

The gas temperature in the laundry was slightly higher in the simulation with steel structures than in the simulation with FRP structures during the first ca. 22 min. This was likely due to better insulation capacity of the steel structures. The gas temperature in the corridor during this period was similar for both simulations. The gas temperatures continued to increase in the simulation with FRP structures as the combusting fuel released heat.

2) Laundry door open

HRR, Tgas_laundry5_z155cm, and Tgas_Corridor2 values from both simulations with the design fire located in the middle of the starboard side and laundry door open are shown in Fig. 4.

Compared to the simulation with all doors closed, the main features of the simulation with the laundry door open were rather similar, though HRR and gas temperature levels were different, and there were some differences in time scales.
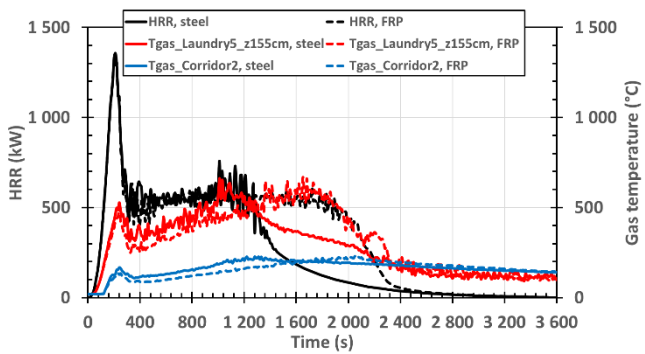
Fig. 4. Simulated HRR and gas temperature results, design fire in the middle of the starboard side, laundry door open.

During the first ca. 1300 s (ca. 22 min) of the simulation, the HRR values were very similar in both simulations. Then, the fire in the simulation with steel as primary bulkhead material began to decay according to the design fire curve. Some delayed combustion of the previously produced fuel gas occurred in the simulation with steel structures, but most of the excess fuel gas had been removed by the ventilation. In the simulation with FRP as the primary bulkhead material, the FRP structures generated gaseous fuel, unable to combust completely due to lack of oxygen. Due to sufficiently high gas temperature in the laundry room, the unburnt gaseous fuel continued to combust after the decay of the design fire.

The gas temperature in the laundry was slightly higher in the simulation with steel structures than in the simulation with FRP structures during the first ca. 22 min. The gas temperature in the corridor was also higher in the simulation with steel structures during the first ca. 1600 s (ca. 27 min), likely due to better insulation capacity of the steel structures. The gas temperatures continued to increase in the simulation with FRP structures as the combusting fuel released heat.

3) Laundry and portside corridor doors open
HRR, Tgas_laundry5_z155cm, and Tgas_Corridor2 values from both simulations with the design fire located in the middle of the starboard side and laundry and portside corridor doors open are shown in Fig. 5.
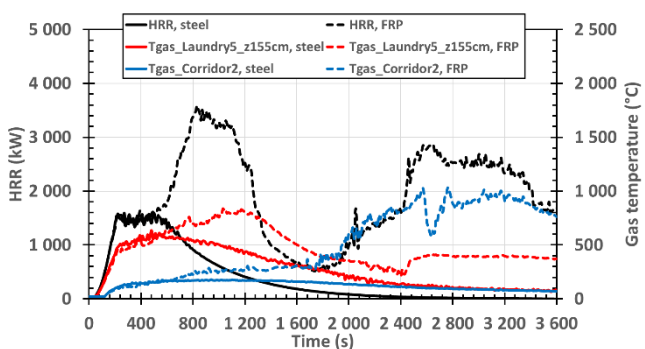

Fig. 5. Simulated HRR and gas temperature results, design fire in the middle of the starboard side, laundry and portside corridor doors open.

Compared to the simulations with all doors closed and with the laundry door open, the case with two doors open showed more differences in HRR and gas temperature levels, and time scales.

During the first ca. 520 s (ca. 9 min) of the simulation, the HRRs were very similar in both simulations. After this, the fire in the simulation with steel as primary bulkhead material began to decay according to the design fire curve. In the

simulation with FRP as the primary bulkhead material, the FRP structures generated gaseous fuel, unable to combust completely due to lack of oxygen. Due to sufficiently high gas temperature in the laundry, the unburnt gaseous fuel continued to combust after the decay of the design fire. The peak in the HRR in the simulation with FRP structures between ca. 500 and 1300 s was caused by the pyrolysis of the first FRP layer of the laundry room bulkheads. The second FRP layer did not pyrolyse at this time, as it was protected by mineral wool. After ca. 1800 s (ca. 30 min), the corridor bulkheads began to burn, which caused a large secondary peak in the HRR.

The gas temperatures in the laundry and the corridor were slightly higher in the simulation with steel structures than in the simulation with FRP structures during the first ca. 9 min, likely due to better insulation capacity of the steel structures. The gas temperatures continued to increase in the simulation with FRP structures as the combusting fuel released heat. When the corridor bulkheads began to burn after ca. 1800 s (30 min), the gas temperature in the corridor rapidly increased.

B. Fire in the aft corner on the portside
1) All doors closed
HRR, Tgas_laundry5_z155cm, and Tgas_Corridor2 values from both simulations with the design fire located in the aft corner on the portside and all doors closed are shown in Fig. 6.
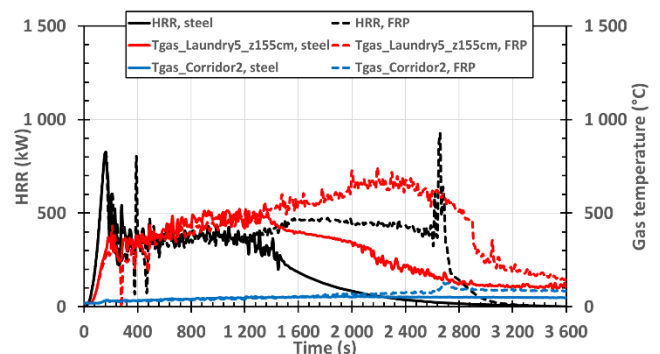

Fig. 6. Simulated HRR and gas temperature results, design fire located in the aft corner on the portside, all doors closed.

As can be seen by comparing Fig. 3 and Fig. 6, the simulation results with different design fire location but the same ventilation conditions were rather similar.

2) Laundry door open
HRR, Tgas_laundry5_z155cm, and Tgas_Corridor2 values from both simulations with the design fire located in the aft corner on the portside and laundry door open are shown in Fig. 7.
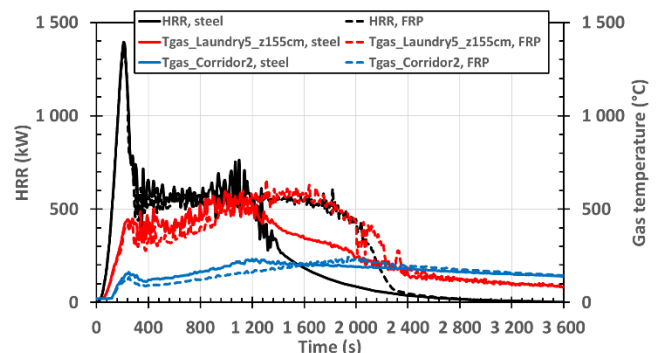

Fig. 7. Simulated HRR and gas temperature results, design fire located in the aft corner on the portside, laundry door open.

Again, by comparison of Fig. 4 and Fig. 7, the simulation results with different design fire location but the same ventilation conditions showed similar features.

3) Laundry and portside corridor doors open
HRR, Tgas_laundry5_z155cm, and Tgas_Corridor2 values from both simulations with the design fire located in the aft corner on the portside and laundry and portside corridor doors open are shown in Fig. 8.
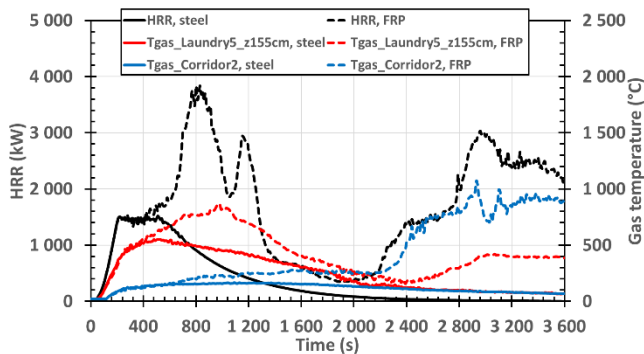

Fig. 8. Simulated HRR and gas temperature results, design fire located in the aft corner on the portside, laundry and portside corridor doors open.

During the first ca. 560 s (ca. 9 min) of the simulation, the HRRs were very similar in both simulations. After this, the fire in the simulation with steel as primary bulkhead material began to decay according to the design fire curve. In the simulation with FRP as the primary bulkhead material, the FRP structures generated gaseous fuel, but it was unable to combust completely due to lack of oxygen. As the gas temperature in the laundry room was sufficiently high, the unburnt gaseous fuel continued to combust after the decay of the design fire. The peak in the HRR in the simulation with FRP structures between ca. 500 and 1300 s was caused by the pyrolysis of the first FRP layer of the laundry room bulkheads. The second FRP layer did not pyrolyse at this time, as it was protected by mineral wool. After ca. 2000 s (ca. 33 min), the corridor bulkheads began to burn, which caused a large secondary peak in the HRR.

The gas temperatures in the laundry and the corridor were slightly higher in the simulation with steel structures than in the simulation with FRP structures during the first ca. 9 min. This was likely due to better insulation capacity of the steel structures. The gas temperatures continued to increase in the simulation with FRP structures as the combusting fuel released heat. After the corridor bulkheads began to burn after ca. 2000 s (ca. 33 min), the gas temperature in the corridor rapidly increased.

The simulation results with different design fire location but the same ventilation conditions were mostly similar with some relatively small differences. The HRRs had some differences between the simulations with different design fire locations, as varying the location caused some alterations to the ventilation. When the design fire was located in the aft corner on the portside, the first large peak had a smaller secondary peak due to temporary lack of oxygen and consequent reduction in the HRR. When the design fire was located in the middle of the starboard side instead, no secondary peak was formed as oxygen was more readily available through the open laundry door. The secondary peak due to the burning of the corridor bulkheads began ca. 200 s (ca. 3 min) later in the simulation with design fire located in the aft corner on the portside than in the simulation with

design fire located in the middle of the starboard side bulkhead due to the differences in ventilation.

IV. DISCUSSION AND CONCLUSION

The objective of this work was to study using FRP as the primary ship construction material from the fire safety aspect. Several fire scenarios inside the superstructure of a 4250 TEU container vessel were simulated, and the utilized design fires, ventilation conditions and bulkhead structures were varied.

The availability of oxygen is the key factor for the HRR. When the HRRs of the fires are the same due to ventilation-controlled conditions, there are only small differences in gas temperatures and other monitored quantities between the simulations with steel and FRP structures. However, when there is more oxygen available in the simulations due to the door open to the outside, there is a significant increase in the HRR especially in the simulations with FRP structures. It was noted that in such cases the corridor bulkheads would begin to burn, causing a second major peak in the HRR.

The simulation results highlight that FRP structures present a significant fire load by themselves, and should be well protected. Early detection and containment of the fire are of high importance for preventing fire spread. In the simulations where the structures were made of FRP instead of steel, the fire durations were significantly longer as there was more fire load available. Longer fire duration in the space of origin increases the risk of fire spreading to adjacent compartments.

The results presented in this paper are valid only for the specific protective solutions studied with the layer thicknesses used in the simulations. The assumptions and modelling choices made in this work should be considered when making extrapolative conclusions from the results presented in this paper.

REFERENCES

[1] K. McGrattan, S. Hostikka, R. McDermott, J. Floyd, C. Weinschenk, and K. Overholt, "Fire Dynamics Simulator Technical Reference Guide Volume 1: Mathematical Model," NIST Special Publication 1018 Sixth Edition. Gaithersburg, Maryland, National Institute of Standards and Technology, 2013, 173 p.

[2] EN 1993-1-2:2005, "Eurocode 3: Design of steel structures. Part 1-2: General rules. Structural fire design," Brussels, European Committee for Standardization, 2005, 78 p.

[3] M. J. Hurley (ed.), "SFPE Handbook of Fire Protection Engineering, Fifth Edition," New York, NY, Springer, 2016.

[4] FIBRESHIP Deliverable D2.4 (WP2), "Report and database on the results of the fire performance experiments," 2018, 46 p. + app. 26 p., http://www.fibreship.eu/wp-content/uploads/2017/07/D24-Report-on-fire-performance-experiments.pdf

[5] A. Matala, "Methods and applications of pyrolysis modelling for polymeric materials", VTT Science 44. Espoo, VTT Technical Research Centre of Finland, 2013, 85 p. + app. 87 p.

[6] ISO 7547:2002, "Ships and marine technology. Airconditioning and ventilation of accommodation spaces. Design conditions and basis of calculations," Geneva, International Organization for Standardization, 2002, 13 p.